World Academy of Science, Engineering and Technology
International Journal of Mechanical and Mechatronics Engineering
Vol:10, No:5, 2016

Computational Investigation of Secondary Flow Losses in Linear Turbine Cascade by Modified Leading Edge Fence

K. N. Kiran, S. Anish

Abstract**—**It is well known that secondary flow loses account about one third of the total loss in any axial turbine. Modern gas turbine height is smaller and have longer chord length, which might lead to increase in secondary flow. In order to improve the efficiency of the turbine, it is important to understand the behavior of secondary flow and device mechanisms to curtail these losses. The objective of the present work is to understand the effect of a stream wise end-wall fence on the aerodynamics of a linear turbine cascade. The study is carried out computationally by using commercial software ANSYS CFX. The effect of end-wall on the flow field are calculated based on RANS simulation by using SST transition turbulence model. Durham cascade which is similar to high-pressure axial flow turbine for simulation is used. The aim of fencing in blade passage is to get the maximum benefit from flow deviation and destroying the passage vortex in terms of loss reduction. It is observed that, for the present analysis, fence in the blade passage helps reducing the strength of horseshoe vortex and is capable of restraining the flow along the blade passage. Fence in the blade passage helps in reducing the under turning by 7^0 in comparison with base case. Fence on end-wall is effective in preventing the movement of pressure side leg of horseshoe vortex and helps in breaking the passage vortex. Computations are carried for different fence height whose curvature is different from the blade camber. The optimum fence geometry and location reduces the loss coefficient by 15.6% in comparison with base case.

Keywords**—**Boundary layer fence, horseshoe vortex, linear cascade, passage vortex, secondary flow.

I. Introduction

DECREASE in the fossil fuel over the recent years motivates on efficiency improvement by decreasing the loss. It is stated that 0.1% improvement in specific fuel consumption was worth around $22k a year on a Boeing 747 [1].

In any gas turbine about one third of the total losses is attributed to secondary flow losses. It is therefore very essential to understand the underlying physics and device mechanics to curtail these losses. Secondary loss is three-dimensional in nature due to the vortical flow structure in the blade passage. Especially gas turbine blade with high camber exhibits flow separation and vorticial structure in the flow.

Secondary flow is always transverse to the primary flow caused due to the cross passage pressure gradient in the boundary layer in the blade passage [2]-[5]. The detailed description of experimental secondary flows feature and effect of boundary layer in a straight turbine cascade are given by Sieverding [6]. Germain [7] defines the secondary flow as an additional flow feature due to the presence of end walls, so it is important to analyze the end wall. The detailed description of secondary flow in the boundary layer and its three-dimensional nature is presented experimentally in [8].

Flow through the turbine is very complex due to three-dimensional nature such as turbulence, pressure gradient and vortices like Horseshoe vortex, corner vortex, end wall vortex, passage vortex and tip vortex. Among these, horseshoe vortex and passage vortex are the major source of losses. Sharma and Butler [9] give the overview of different vortex structures on cascade end wall (Fig. 1).

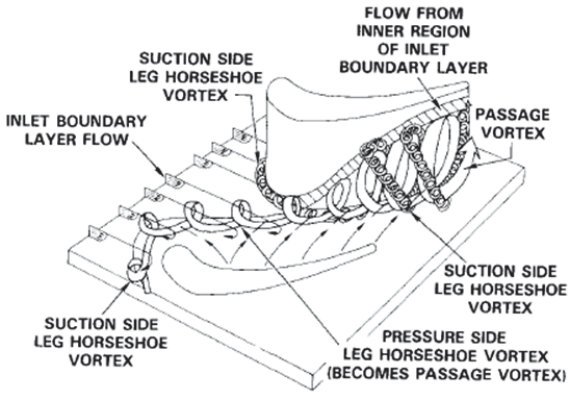

Fig. 1 Cascade end wall flow [9]

Horseshoe vortex can be suppressed by sharp leading edge and size of horseshoe vortex depends on incidence angle [10]. The suction side leg vortex (S_p) and pressure side leg vortex (H_p) meet together in the mid-passage region where the two separation lines exist in the passage merge. This occurs close to the suction side of blade, and merger of the two vortices forms a stronger vortex known as passage vortex [11]. As the pressure side leg vortex is much stronger compared to suction side vortex when they meet, the sense of rotation of passage is considered by sense of rotation of pressure side leg vortex. The passage vortex is primary responsible for total pressure loss in the secondary flow region near the suction side of blade.

K. N. Kiran is with the National Institute of Technology, Karnataka, Pin – 575025, India (phone: +91- 9945583068; e-mail: kirankn24@gmail.com).

S. Anish, Assistant Professor, is with the Department of Mechanical Engineering, National Institute of Technology, Karnataka, Pin – 575025, India (e-mail: anish@nitk.edu.in).

A. Overview of Previous Work

There are many methods to reduce secondary flow losses in turbine cascade like leading edge filleting, stream-wise end wall fence on the end wall and blade surface, end wall contouring, end wall film injection [12], [13], blade thickening in the end wall region, blade lean [14], [15] and sweep etc.

Filleting the blade leading edge-end wall juncture helps in reducing the intensity of horseshoe vortex [16]-[18]. The fillet design effectively accelerates the boundary layer thereby migrates the effect of total pressure gradient. By creating the strong suction side horseshoe vortex by leading edge modification, which ensures by weakening the counter rotating passage vortex [19].

Another method in controlling the flow feature near the end wall boundary layer is end wall contouring [1], [7], [9]. There are two ways of end wall profiling – axial profiling along the passage with no pitchwise variation [20] and non-axisymmetric profiling along the passage in both axial and pitchwise direction [21]-[23]. The profiling assists in accelerating the boundary layer fluid at the end wall and reduce pitchwise pressure gradient. The novel feature of secondary flow with end wall profiling of equal peak and dip value is examined [24].

One of the simplest and powerful tool in the minimization loss is fencing [2], [25]. Fence effectively helps in reducing the intensity of loss core leading to lesser aerodynamic losses in turbine passage [26], [27]. It is found that fences are more effective if $1/3^{rd}$ of inlet boundary layer thickness high and it is placed at half the blade pitch [25]-[28]. With the usage of fence, the accumulation of low energy fluid is reduced, which results in an improved aerodynamic lift coefficient [28]. However, at higher mass flow rates, fence may add disturbance to the passage flow and increase the loss coefficients, if not properly designed.

The objective of the present work is to investigate computationally the effect of leading edge modification of end wall fence in a linear turbine cascade. The optimum fence geometry and location is decided by measuring the loss coefficient and flow turning. The leading edge of fence is modified in order to break the horseshoe vortex. This novel design is expected to reduce the amount of low energy boundary layer fluid that is convicted by passage vortex thereby reduce the losses in the passage.

II. Methodology

A. Blade Profile Geometry

The Durham cascade is a low speed, large scale linear cascade for a high pressure rotor design. The blades are designed to have an aerodynamic similarity same as real machines rather than geometrical similarity. The blade profile and geometrical details are shown in Fig. 2 [12] and Table I. The Durham cascade has already been subjected to numerous study on end wall contouring and filleting the leading edge [18], [22]. In this study, an attempt is made by incorporating the unique geometry of fence in the Durham cascade.

B. Design Study

Domain consists of single blade which is placed exactly at one pitch distance and fence is positioned at fixed distance from the blade camber line as shown on Fig. 3. Fence is exactly half the pitch from the blade camber line and curvature of fence do not follow the blade camber towards the leading edge of blade. Modified fence starts from 11% C_{ax} move straight along axial direction up to 42% C_{ax}. From 42% C_{ax} fence curvature flow same as blade camber curvature till the trailing edge. Thickness of the fence is 2.5mm from leading edge to trailing edge. The investigation was carried out for four different fence height named for convenience as shown in Table II.

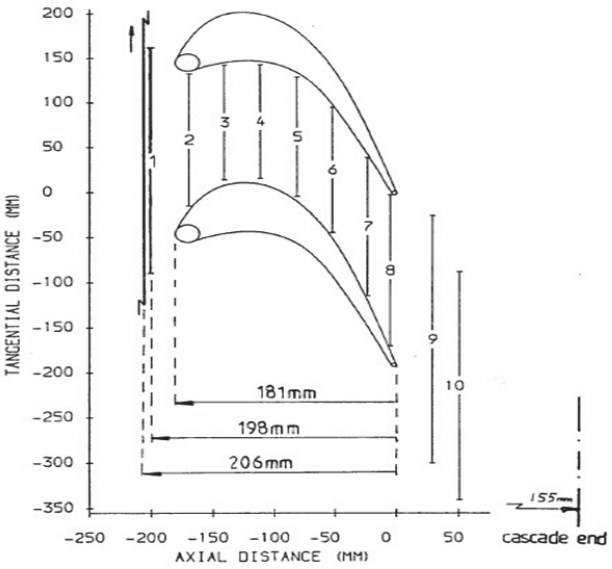

Fig. 2 Blade Profile and Measurement Location [12]

TABLE I
CASCADE BLADE DETAILS

Blade Inlet Angle	47.6^0
Flow Inlet Angle	62.6^0
Blade Exit Angle	-68.0^0
Flow Exit Angle	-68.8^0
Stagger Angle	-36.1^0
Blade Chord	224 mm
Axial Chord	181 mm
Blade Pitch	191 mm
Blade Span	400 mm
Reynolds Number (axial chord and exit velocity)	4.3×10^5
Exit Mach Number	0.11

mm = millimeter.

In the current study geometrical model for blade profile is done using solid works and flow domain and meshing is done in ICEM-CFD 15. The domain geometry consists of inlet which is at 1.5 times the axial chord and outlet at distance of 2times the axial chord from the leading edge of blade. The domain was generated for half the span of blade in radial direction by defining symmetry and translational periodicity along the transverse direction at one pitch length shown in Fig.

3. The mesh around the blade, hub and fence surface is fully structured and remaining flow domain is unstructured in axial and tangential direction. The maximum size of mesh size for whole domain is 3.5 mm with scale factor of 1. The prism layers are attached around the blade and hub surface to study the boundary layer effects of flow. The grid independence study was carried out and solution was found to be grid independent at 2.2 million. The cell height is 0.35 mm (first cell height normal to the surface) with exponential height ratio of 1.15 up to 12 layers.

C. Solver Details

ANSYS-CFX was used for computational simulation in current study with transition SST k-ω model to model the turbulence. The transition SST k-ω turbulence model was found to be most suitable for analysis of secondary flows [2], [29]. The transition SST model is based on standard SST k-ω equation with fully turbulence. The inlet boundary condition is velocity of 19.1 m/s along the flow direction, turbulence intensity of 5% and static temperature of 292.15 K. At the outlet ambient conditions and the symmetric boundary conditions at mid-span was specified. All the walls are given as no slip condition and adiabatic boundary condition. The current study was done using air as working fluid on single blade passage with translational periodic boundary condition at one pitch length on either sides. High resolution discretization scheme was chosen for all calculations and convergence criteria is set to 10^{-6} for all variables.

TABLE II
DETAILS OF FENCE HEIGHT

SL. no	Case no.	Fence Height
1	Case-0 (base case)	0 mm
2	Case-1	10 mm
3	Case-2	20 mm
4	Case-3	30 mm
5	Case-4	40 mm

mm = millimeter.

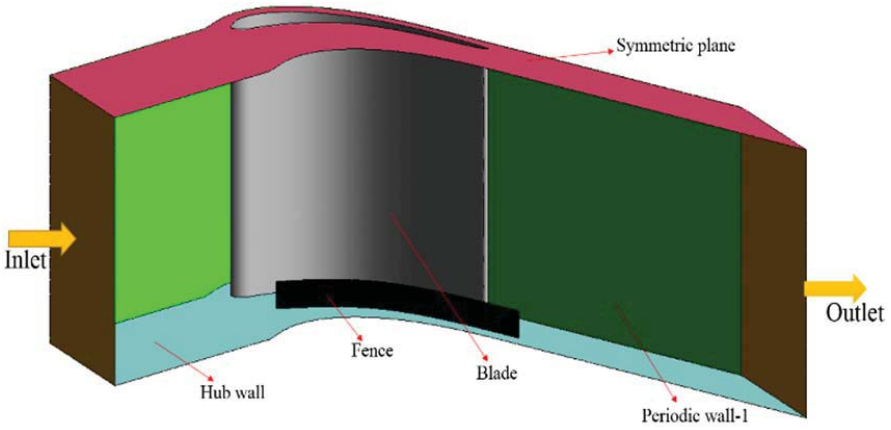

Fig. 3 Typical Computational domain with blade and fence

III. RESULTS AND DISCUSSIONS

A. Validation

The CFD investigation is carried out for base case (without fence) on Durham cascade with single blade and compared with the experimental results by Biesinger [12]. The inlet velocity is specified as 19.1 m/s along the flow direction with turbulence intensity of 5% and at the outlet relative pressure is set as zero. Translational periodic boundary condition is used at exactly one pitch. The static pressure coefficient (C_p) value is defined as (1):

$$C_p = \frac{P_1 - P}{1/2 \rho V_1^2} \quad (1)$$

The static pressure coefficient variations are plotted at 53.5 mm from the end wall and compared with experimental values [12] as shown in Fig. 4. Computations are carried out for three different turbulence model the SST-Transition, k-epsilon and k-omega. Static pressure plots qualitatively and quantitatively follow the experimental results for all the three turbulence model. It is also observed that from 150 mm axial chord towards the trailing edge pressure coefficient is reduced due to flow separation. Near the trailing edge a point of inflection is observed due adverse pressure gradient in the flow.

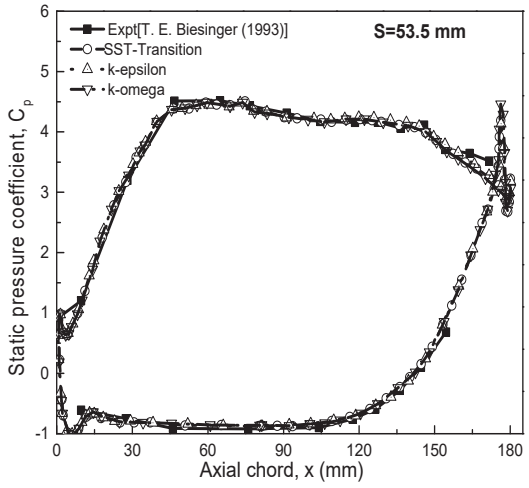

Fig. 4 Blade static pressure distribution at 53.5 mm spanwise distances from the endwall

B. Total Pressure Loss Coefficient

In the current study, computational investigations of secondary flows in a linear turbine cascade are presented. Detailed analyses of losses with fence and without fence are carried out. The primary objective is to understand the effect of fence on the secondary flow losses. The loss coefficients are evaluated from the mid-span of blade to hub wall. The pitch mass averaged total pressure loss coefficient along the span of blade at 128% axial chord (C_{ax}) is calculated for all the cases. The pitch mass averaged total pressure loss coefficient ($\overline{C_{P0}}$) is calculated from (2),

$$\overline{C_{P0}} = \frac{\int V_u \xi dT}{\int V_u dT} \quad (2)$$

where, ξ(zeta) is

$$\xi = \frac{P_{01} - P_0}{\rho V_1^2/_2} \quad (3)$$

The numerical solution for the pitch mass averaged total pressure loss coefficient for four different fence height in comparison with the base case are shown in Fig. 5. The coefficient of pressure losses is more near the end wall for fence cases in comparison with base case. It is observed that the value of loss coefficients rapidly decreases from the end wall up to a span of 40 mm. There is a slight increase in the value of loss coefficient from 40 mm to 70 mm for all fence cases except for case-1 (10 mm fence height). The peak loss coefficient occurs from 70 mm to 90 mm distance from the end wall position and from then on there is decrease in the value of loss coefficient. These variations suggest that the presence of fence is very effective in breaking down the passage vortex even though it increases the loss near the end wall. However, pitchwise mass averaged total pressure loss has come down for all the fence cases (except case-1) in comparison with no fence case. The intensity of passage vortex has come down in the presence of fence due to breaking of passage vortex by fence in the blade passage. For the base case, loss coefficient has increased significantly from 80 mm of span indicating intensified passage vortex. Loss coefficient almost remains constant from 100 mm to half blade span for all fence cases. It is also observed that as the height of fence increases the loss coefficient near the end wall increases. For the case-1 (10 mm fence height), the loss has increased beyond the base case. This is due to the fact that fence height is not sufficient to break the horseshoe vortex while it acts as obstacle in flow which creates turbulence.

The variation of mass averaged total pressure loss coefficient ($\overline{\overline{C_{P0}}}$) through the measuring planes from 50% axial chord (C_{ax}) to 150% C_{ax} is shown in Fig. 6. The trailing edge of blade is 100% C_{ax}. The variation of $\overline{\overline{C_{P0}}}$ along the axial direction is qualitatively similar for all the computations. It was also observed that $\overline{\overline{C_{P0}}}$ increases almost linearly after the trailing edge of blade for the base case. This sudden increase is due to mixing of fluid from pressure and suction side of blade after the trailing edge. However, with the presence of fence, the $\overline{\overline{C_{P0}}}$ variation is much more horizontal (smaller slope) than the base case. Comparing the results of mass averaged $\overline{\overline{C_{P0}}}$ for different fence height it was found that there is an optimum fence height (i.e. fence height = 30 mm) beyond which the loss increases. For case-1 (fence height=10 mm) the loss coefficient has increased by 52% in comparison with base case. For the case-2 it is observed that there is reduction in loss by 15.63% at 128% C_{ax} in comparison with base case. It is also observed that loss coefficient is more for case-2 in the blade passage (before trailing edge) in comparison with case-4. Downstream from the trailing edge the loss coefficient for case-4 is higher in comparison with case-2. This is due to fact that demolished vortex crosses the fence in case-2 because of insufficient fence height. This is observed in stream lines in the blade passage.

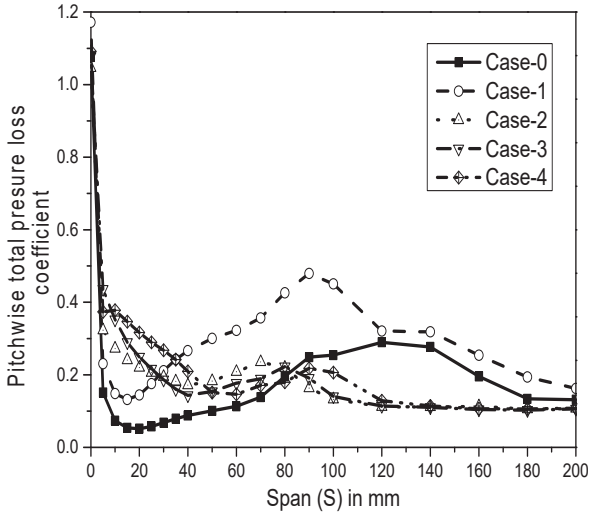

Fig. 5 Pitchwise mass averaged total pressure loss coefficient ($\overline{C_{P0}}$) along the span of blade at 128% C_{ax}.

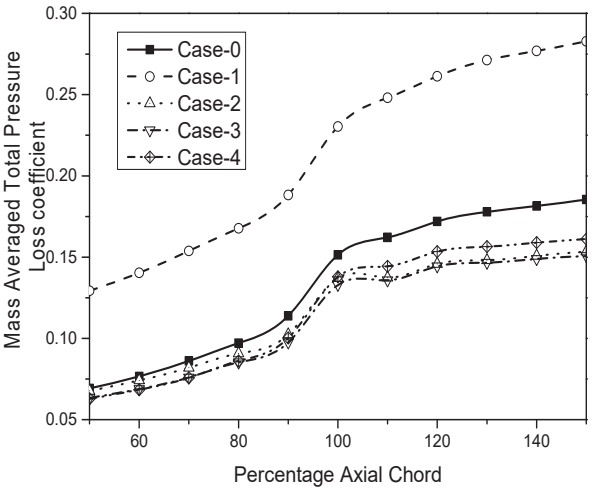

Fig. 6 Mass averaged total pressure loss coefficient ($\overline{\overline{C_{P0}}}$) along axial direction

C. Effect of Underturning and Overturning

The aim of the design was primarily to reduce underturning and overturning at the exit, which improves the performance

of succeeding blade row. Fig. 7 shows the exit flow angle for all the simulated cases along the spanwise direction at 128% C_{ax}. The pitch mass averaged exit flow angle is calculated from (4),

$$\bar{\alpha} = Tan^{-1}\left(\frac{\overline{V_v}}{\overline{V_u}}\right) \quad (4)$$

As the pressure leg of horseshoe vortex moves towards the suction side of blade in the blade passage merges with counter rotating vortex and forms a passage vortex. This results in a change in the flow angle and work output. This turning of the fluid is to balance the static pressure gradient and centrifugal force. To maintain the radial equilibrium, the flow near the mid span is considered to be two-dimensional with streamwise and tangential pressure gradient. On the contrary, near the end wall boundary layer, flow is three-dimensional with spanwise velocity gradient along with streamwise and tangential direction. The pressure gradient for the flow deviation can be obtained from (5) [30],

$$\frac{P_{ps}-P_{ss}}{pitch} \approx \frac{dp}{dr} = \rho\frac{V_{MS}^2}{r_{MS}} = \rho\frac{V_{BL}^2}{r_{BL}} \quad (5)$$

where, V_{MS} is velocity in the mid span flow and r_{MS} is the radius of curvature of the stream line in the mid-span. And subscript BL indicates boundary layer flow.

Near the end wall, velocity of fluid decreases in the boundary layer region and radius of curvature is less for boundary layer flow. There exists a pressure difference along the span which results in over-turning in the passage flow. The "overturning" refers to larger flow deflection than expected geometrical deflection. Similarly, if flow deflection is less than geometrical deflection of blade, then it is "under turning". In Fig. 7, near the end wall, flow will be overturning up to 30 mm span for cases with fence. Averaged angle of underturning is about 4^0 is at 40-80 mm from the end wall for fence cases-2, 3, and 4. The intensity of loss core is high in the underturning zone for all the cases, but the underturning is weakened by fences. By influence of fence under turning and overturning, it decays faster towards the midspan direction in comparison with base case. From the end wall (S=100 mm) fluid follows almost the blade exit angle up to mid span of the blade. In comparison with no fence case, fence cases have lower underturning and overturning along the span of blade. By increasing the height of the fence beyond the optimum fence height, fence acts as blade, which leads to more over and under turning of flow. Case-1 shows the adverse effect on the flow turning in comparison with other cases. Therefore, the effect of optimum fence clearly shows reduction in the passage vortex in terms of reduced flow turning at the exit of blade.

D. Effect on Coefficient of Secondary Kinetic Energy (CSKE)

Fig. 8 shows the pitch mass averaged CSKE results, and the assessment of losses with and without fence along the span was measured at 128% C_{ax}. CSKE is calculated by using the following correlation (6)-(8),

$$CSKE = \frac{SKE}{\rho V_1^2/_2} \quad (6)$$

where,

$$SKE = \frac{1}{2}\rho(V_{sec}^2 + V_w^2) \quad (7)$$

and

$$V_{sec} = -V_u sin\alpha_2 + V_v cos\alpha_2 \quad (8)$$

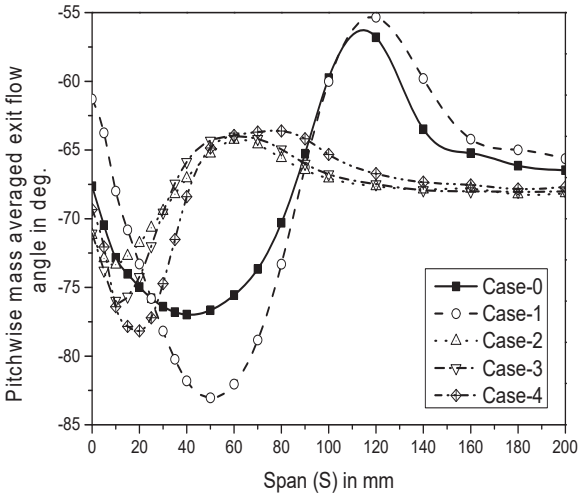

Fig. 7 Pitchwise averaged exit flow angle along the span

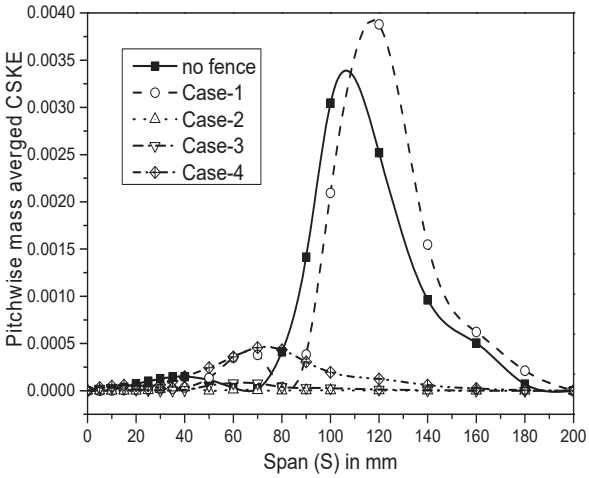

Fig. 8 Pitchwise mass averaged Coefficient of secondary kinetic energy (CSKE) at 128% C_{ax} along the span

Secondary kinetic energy (SKE) at any plane measures vortices caused due to viscous effect and potential flow. For in-viscid flow, SKE is propositional to the square of length of the vortex; i.e., when the mean flow increases, SKE of a streamwise vortex increases [4].

It is observed from Fig. 8 that maximum CSKE is at 100 mm from the end wall for base case. For cases with fence (except case-1), the loss has been reduced which is signified by lower area under the curve. Case-2 has the least area under

the curve in comparison with other fence cases. The hump and dip in all the curves in Fig. 8 near the endwall signifies the intensity of corner vortex. The peak of loss core shift near the end wall by increasing the height of fence. For increase or decrease in the fence height other than case-2 and case-3, the loss increases. The development and propagation of passage vortex is prevented by the fence which results in low CSKE.

E. Overall Effect of Fence

The mass averaged total pressure loss coefficient C_{P0} counters are plotted at 128% C_{ax} and compared with base case and fence cases are shown in Figs. 9 (a)-(e). S represents the span direction of blade and T represents the pitch direction in the cascade. It is observed for base case that loss core is concentrated at one fourth of blade height from the end wall. This is due to radial movement of passage vortex from the end wall. The radial migration of passage vortex is due to fact that the low energy fluid in the boundary layer extracts energy from the midstream flow. This radial migration of vortex disturbs the flow away from the end wall. Thus, overall loss coefficient increased for the base case. In case of fence, the fence helps in breaking down the passage vortex which is main cause of secondary losses. With the incorporation of fence, the loss coefficient has increased near the end wall for all fence cases in comparison with base case. The intensity of passage vortex has reduced for the fence cases except for case-1 in comparison with the base case. For the case-3, the overall loss coefficient at 128% C_{ax} has come down by 15.63% in comparison with the base case. In case-1, the fence height is not sufficient to break the vortex, instead fence creates the turbulence which is the cause of increase in loss value by 52.18%.

Figs. 10 (a) and (b) show the 3D stream lines near the end wall for both fence and no fence case. It is observed from Fig. 10 (a) that the fluid near the end wall move from pressure side to suction side of next blade. This transverse movement is due to the pitchwise pressure gradient. As the fluid proceeds downstream in the blade passage low energy fluid near the end wall move to the mid-stream flow. This is the main cause for radial migration of passage vortex to the midstream flow. By the influence of fence in the blade passage, the flow is stabilized in comparison with base case as seen in Fig. 10 (b). Fence helps in breaking down the passage vortex and avoids the cross flow near the end wall boundary layer, and flow is stabilized in the downstream direction in comparison with base case.

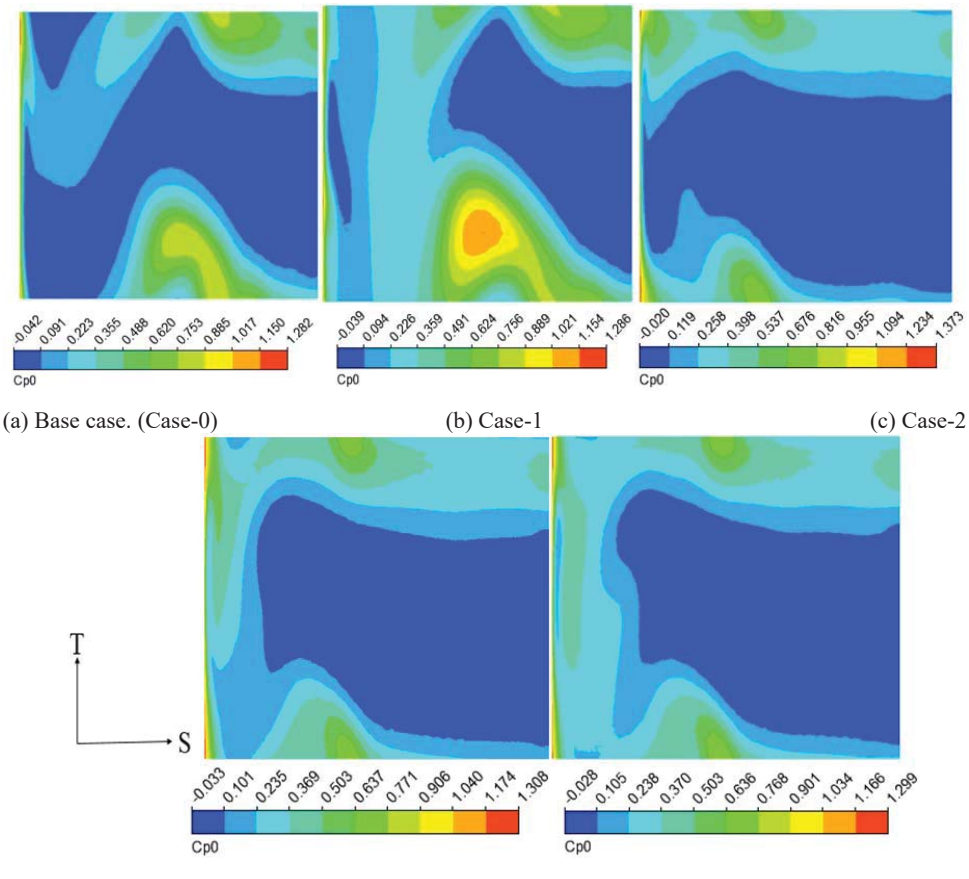

(a) Base case. (Case-0) (b) Case-1 (c) Case-2

(d) Case-3 (e) Case-4

Fig. 9 (a)-(e) Total Pressure loss contours at 12.8% C_{ax}

IV. Conclusion

The conclusions are based on the present investigations on the effect of modified fence leading edge and fence height on the secondary flow losses are.

1. Modified leading edge of fence is successful in breaking down the horseshoe vortex in the blade passage.
2. The magnitude of total pressure loss coefficient and spanwise penetration of passage vortex is reduced by 15.63% for the optimum fence in comparison with the base case.
3. By the influence of fence, the intensity of passage vortex is diminished in the downstream of blade.
4. The flow overturning displaces the underturning peak towards the end wall, results in no turning of flow away from the endwall.
5. The spanwise penetration of vortex core is reduced which is witnessed in the CSKE value.
6. Fence is effective in preventing the cross flow and weakening the vortices near the end wall is observed in 3D streamlines.

Overall it could be concluded that optimum fence helps in reducing the secondary flow losses and improves the performance in the turbine cascade.

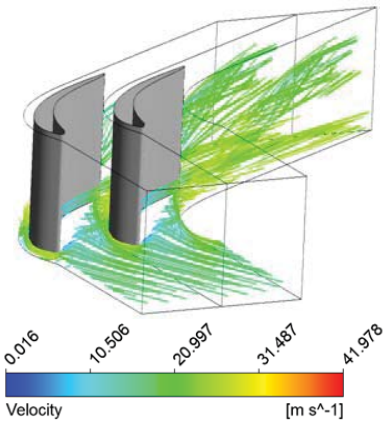

(a) Base case. (Case-0)

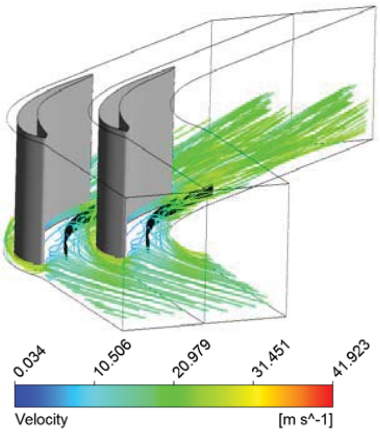

(b) Fence case. (Case-2)

Fig. 10 (a), (b) 3D streamlines near the end wall

Nomenclature

C_{ax}	Axial Chord
C_{P0}	Total pressure loss coefficient
C_P	Static Pressure loss coefficient
CSKE	Coefficient of Secondary kinetic energy
P	Static Pressure
P_0	Total Pressure
H_p	Pressure side leg horseshoe vortex
Re	Reynolds number
S	Blade span direction
S_p	Suction side leg horseshoe vortex
SKE	Secondary kinetic energy
SST	Shear Stress Transport
T	Transverse direction
V	Velocity
V_u	Axial velocity
V_v	Tangential velocity
V_w	Radial velocity
Greek Symbols	
α	Exit flow angle
ρ	Density
Subscripts and superscripts	
1	Inlet of cascade
2	Outlet of cascade
$-$	Pitch-wise mass averaged quantity
$=$	Mass averaged quantity

References

[1] M. G. Rose, "Non-axisymmetric endwall profiling in the HP NGV's of an axial flow gas turbine," In *ASME 1994 International Gas Turbine and Aeroengine Congress and Exposition* (pp. V001T01A090-V001T01A090). American Society of Mechanical Engineers, Jun 1994.

[2] K. N. Kumar, and M. Govardhan, "Secondary Flow Loss Reduction in a Turbine Cascade with a Linearly Varied Height Streamwise Endwall Fence," *International Journal of Rotating Machinery*, *2011*.

[3] R. E. Brachmanski, R. Niehuis, and A. Bosco, "Investigation of a Separated Boundary Layer and its Influence on Secondary Flow of a Transonic Turbine Profile," In *ASME Turbo Expo 2014: Turbine Technical Conference and Exposition* (pp. V02CT38A022-V02CT38A022). American Society of Mechanical Engineers, Jun 2014.

[4] J. D. Denton, "Loss mechanisms in turbomachines." In *ASME 1993 International Gas Turbine and Aeroengine Congress and Exposition* (pp. V002T14A001-V002T14A001). American Society of Mechanical Engineers, May 1993.

[5] L. S. Langston, "Secondary flows in axial turbines—a review," *Annals of the New York Academy of Sciences*, *934*(1), 11-26, 2001.

[6] C. H. Sieverding, "Recent progress in the understanding of basic aspects of secondary flows in turbine blade passages," *Journal of Engineering for Gas Turbines and Power*, *107*(2), 248-257, 1985.

[7] T. Germain, M. Nagel, and R. D. Baier, "Visualisation and Quantification of Secondary Flows: Application to Turbine Bladings with 3D-Endwalls," In *Paper ISAIF8-0098, Proc. of the 8th Int. Symposium on Experimental and Computational Aerothermodynamics of Internal Flows,* Lyon, July 2007.

[8] M. Govardhan, and P. K. Maharia, "Improvement of Turbine Performance by Streamwise Boundary Layer Fences," *Journal of Applied Fluid Mechanics*, *5*(3), 113-118, 2012.

[9] O. P. Sharma, and T. L. Butler, "Predictions of endwall losses and secondary flows in axial flow turbine cascades," In *ASME 1986 International Gas Turbine Conference and Exhibit* (pp. V001T01A098-V001T01A098). American Society of Mechanical Engineers, June 1986.

[10] J. Moore, and A. Ransmayr, "Flow in a turbine cascade: Part 1—Losses and leading-edge effects," *Journal of Engineering for Gas Turbines and Power*, *106*(2), 400-407, 1984.

[11] S. Acharya, and G. I. Mahmood, "Turbine Blade Aerodynamics," *The Gas Turbine Handbook*, *1*, Chapter 4.3, pp. 364-380, 2006.

[12] T. E. Biesinger, "*Secondary flow reduction techniques in linear turbine cascades,"* Doctoral dissertation, Durham University, England, 1993.

[13] N. V. Aunapu, R. J. Volino, K. A. Flack, and R. M. Stoddard, "Secondary flow measurements in a turbine passage with endwall flow modification," *Journal of turbomachinery*, *122*(4), 651-658, 2000.

[14] N. X. Chen, Y. J. Xu, and W. G. Huang, "Straight-leaned blade aerodynamics of a turbine nozzle blade row with low span-diameter ratio,". Journal *of Thermal Science*, *9*(1), 51-62, 2000.

[15] W. Han, H. Huang, and Z. Wang, "Influence of blade chordwise lean on development of cascade losses," *Journal of Thermal Science*, *5*(4), 223-230, 1996.

[16] G. A. Zess, and K. A. Thole, "Computational design and experimental evaluation of using a leading edge fillet on a gas turbine vane," In *ASME Turbo Expo 2001: Power for Land, Sea, and Air* (pp. V003T01A083-V003T01A083). American Society of Mechanical Engineers, June 2001.

[17] M. Hoeger, U. Schmidt-Eisenlohr, Gomez, SOPHIE, H. Sauer. ELMU T, and R. Müller, "Numerical simulation of the influence of a fillet and a bulb on the secondary flow in a compressor cascade," *Task Quarterly*, *6*(1), 25-37, 2002.

[18] S Mank, L. Duerrwaechter, M. Hilfer, R. Williams, S. Hogg, and G. Ingram, "Secondary Flows and Fillet Radii in a Linear Turbine Cascade," In *ASME Turbo Expo 2014: Turbine Technical Conference and Exposition* (pp. V02CT38A011-V02CT38A011). American Society of Mechanical Engineers, June 2014.

[19] H. Sauer, R. Muller, and K. Vogeler, "Reduction of secondary flow losses in turbine cascades by leading edge modifications at the endwall," *Journal of turbomachinery*, *123*(2), 207-213, 2001.

[20] G. Ingram, D. Gregory-Smith, and N. Harvey, "The benefits of turbine endwall profiling in a cascade," *Proceedings of the Institution of Mechanical Engineers, Part A: Journal of Power and Energy*, *219*(1), 49-59, 2005.

[21] G. Brennan, N. W. Harvey, M. G. Rose, N. Fomison, and M. D. Taylor, "Improving the efficiency of the trent 500-hp turbine using nonaxisymmetric end walls—part I: Turbine design," *Journal of turbomachinery*, *125*(3), 497-504, 2003.

[22] N. W. Harvey, M. G. Rose, M. D. Taylor, S. Shahpar, J. Hartland, and D. G. Gregory-Smith, "Non-Axisymmetric Turbine End Wall Design: Part I—Three-Dimensional Linear Design System," In *ASME International Gas Turbine and Aeroengine Congress and Exhibition* (pp. V001T03A049-V001T03A049). American Society of Mechanical Engineers, June 1999.

[23] J. C. Hartland, D. G. Gregory-Smith, N. W. Harvey, and M. G. Rose, "Non-Axisymmetric Turbine End Wall Design: Part II—Experimental Validation," In *ASME International Gas Turbine and Aeroengine Congress and Exhibition* (pp. V001T03A050-V001T03A050). American Society of Mechanical Engineers, June 1999.

[24] G. Ingram, D. Gregory-Smith, and N. Harvey, "Investigation of a novel secondary flow feature in a turbine cascade with end wall profiling," *Journal of turbomachinery*, *127*(1), 209-214, 2005.

[25] Y. J. Moon, and S. R. Koh, "Counter-rotating streamwise vortex formation in the turbine cascade with endwall fence," *Computers & fluids*, *30* (4), 473-490, 2001.

[26] T. Kawai, S. Shinoki, and T. Adachi, "Secondary flow control and loss reduction in a turbine cascade using endwall fences," *JSME international journal. Ser. 2, Fluids engineering, heat transfer, power, combustion, thermophysical properties*, *32*(3), 375-387, 1989.

[27] T. Kawai, "Effect of Combined Boundary Layer Fences on Turbine Secondary Flow and Losses," *JSME International Journal Series B Fluids and Thermal Engineering*, *37*(2), 377-384, 1994.

[28] M. Govardhan, A. Rajender, and J. P. Umang, "Effect of stream wise fences on secondary flows and losses in a two-dimensional turbine rotor cascade," *Journal of Thermal Science*, *15*(4), 296-305, 2006.

[29] D. Dunn, G. C. Snedden, and T. W. Von Backström, "Turbulence model comparisons for a low pressure 1.5 stage test turbine," *19th Conference of the International Society for Air Breathing Engines*, Montreal, Quebec, Canada, pp 7, Sept 2009.

[30] R. Saha, "Aerodynamic Investigations of a High Pressure Turbine Vane With Leading Edge Contouring at Endwall in a Transonic Annular Sector Cascade," *Licentiate Thesis*, KTH School of Industrial Engineering and Management, 2012.